Synthetic Metals 162 (2012) 236–239

Contents lists available at SciVerse ScienceDirect

Synthetic Metals

journal homepage: www.elsevier.com/locate/synmet

Synthesis, characterization and physical properties of a novel xanthan gum/polypyrrole nanocomposite

Hamid Heydarzadeh Darzi, Saeedeh Gilani Larimi*, Ghasem Najafpour Darzi

Babol University of Technology, P.O. Box 484, Babol, Iran

ARTICLE INFO

Article history:
Received 31 October 2011
Received in revised form
30 November 2011
Accepted 1 December 2011
Available online 23 December 2011

Keywords:
Polypyrrole
Xanthan gum
Nanocomposite
Physical property
Chemical structure

ABSTRACT

Polypyrrole/xanthan gum nanocomposite was synthesized by oxidative polymerization of pyrrole in presence of xanthan gum. The atomic force microscopy (AFM) and Fourier transform infrared (FT-IR) measurements confirm the morphology and structure of synthesized nanocomposite. The nanocomposites particles size were obtained from 58 to 98 nm. Also, the surface roughness parameters measured using tapping mode method showed the surface roughness of polypyrrole based nanocomposite extremely affected by xanthan gum. Thermogravimetric analyzer (TGA) curves revealed that xanthan gum can decrease the weight loss of nanocomposite and increase the thermal stability of synthesized nanocomposite as the remained ash amount is improved from 5 to 28%. Also it is found that xanthan gum could enhance the electrical conductivity up to 0.904 S/cm.

© 2011 Elsevier B.V. All rights reserved.

1. Introduction

Composites of carbohydrates and conducting polymers have been a subject of comprehensive research because of showing good biocompatible and physiochemical properties [1,2]. Various substances have been used to form composite from carbohydrates and conducting polymers such as chitosan-polyaniline and carboxymethyl cellulose-polypyrrole [3–6]. One of the well known natural sourced water soluble carbohydrates is xanthan gum that is prepared by *Xanthomonas campestris*. Xanthan gum (XG) is a hetero-polysaccharide with repeated pentasaccharide units consists of two molecular structures of glucose, mannose and one unit of glucuronic acid [7,8]. The presences of organic acids in xanthan gum structure make an anionic polysaccharide sort. Also, interaction of xanthan gum with other polymer molecules may generate a complex structure of them [9]. Biocompatibility and water solubility of xanthan gum introduce it a suitable material for many applications such as food industries, cosmetics and petroleum industries as an emulsifier, stabilizer and viscose agent [10]. However, xanthan gum has limited physiochemical properties like electrical conductivity and thermal stability [9,11]. Polypyrrole (PPy) is a most noted conducting polymer that was considered intensively due to its unique physical properties [12,13]. The electrical conductivity, ion exchange capacity, hydrophobic character and adsorption ability of molecular and macromolecular species cause polypyrrole to use for various purposes; coatings, protein carriers, supercapacitance, gas sensors, etc. [14–17]. On the other hand, two facts that restrict the applications of polypyrole are insolubility of it in common solvents and its limited biocompatibility [18–20]. Production and characterization of polypyrrole nanocomposite have been investigated in other literatures but the synthesis and physical properties of polypyrrole–xanthan gum nanocomposite has not been studied yet [21]. In this study, polypyrrole–xanthan gum nanocomposite was prepared in the aqueous solution using APS (ammonium peroxydisulfate) as an oxidant. The morphology and structure of produced nanocomposite were analyzed by atomic force microscopy (AFM) and Fourier transform infrared (FT-IR) respectively. In addition, electrical conductivity and thermal stability of synthesized nanocomposite were considered for different composition.

2. Experimental

2.1. Instruments and materials

The atomic force microscopy (AFM) (Nanosurf scanning probe-optical microscope, EasyScan II, Swiss), the Fourier transform infrared (FT-IR) spectrometer spectra in the range 500–4000 cm^{-1} (Shimadzu model 4100, Japan), A standard four-probe method using a Keithley 196 System DMM Digital Multi-meter and an Advantest R1642 programmable dc voltage/current generator as

* Corresponding author. Tel.: +98 9112182926; fax: +98 1113234204.
E-mail address: saeedeh_gilani@yahoo.com (S.G. Larimi).

0379-6779/$ – see front matter © 2011 Elsevier B.V. All rights reserved.
doi:10.1016/j.synthmet.2011.12.004

Table 1
Preparation conditions, conductivity and particle size of synthesized nanocomposites.

Nanocomposite No.	XG (g)	Pyrrole (mol)	Oxidant (APS) (mol)	Average particle size (nm)	Conductivity (S/cm)
Pure PPy	–	0.2	0.25	120	0.537
1	1	0.2	0.25	98	0.680
2	2	0.2	0.25	80	0.904
3	3	0.2	0.25	71	0.710
4	4	0.2	0.25	65	0.092
5	5	0.2	0.25	58	0.025
Pure XG	–	–	–	43	0.008

the current Source and thermo gravimetric analyzer (TGA) (Perkin Elmer model 4000, USA) were employed.

In this work pyrrole, distilled under reduced pressure prior to use, ammonium peroxydisulfate (APS $(NH_4)_2S_2O_8$), hydrochloric acid (Merck, Germany), deionized water and xanthan gum ($Mw = 2 \times 10^6$) were used.

2.2. Synthesis of polypyrrole

Polypyyrole was synthesized using classical oxidative polymerization of pyrrole dissolved in aqueous HCl (1 M) in the presence of ammonium peroxydisulfate (APS) as the oxidant at ice temperature. Based on literature 0.2 mol of pyrrole was dissolved in 1000 ml of aqueous solution of HCl (1 M) and 0.25 mol ammonium peroxydisulfate was dissolved in 1000 ml HCl (1 M) separately. [21,22].

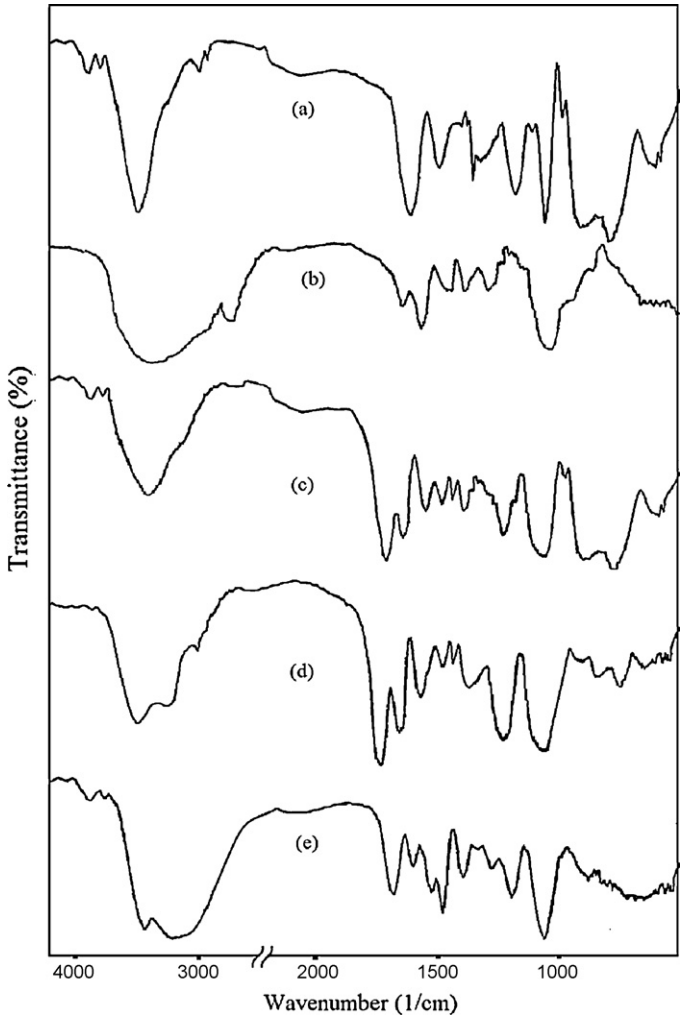

Fig. 1. FT-IR spectra of PPy (a), XG (b), nanocomposite No. 1 (c), No. 2 (d) and No. 3 (e).

2.3. Synthesis of polypyrrole–xanthan gum nanocomposite

The same procedure was used as polypyrrole, however the oxidant solution was prepared in presence of xanthan gum. Ammonium peroxydisulfate and xanthan gum was dissolved in 1000 ml HCl (1 M). The prepared mixture of xanthan gum and oxidant was added slowly to the acidic pyrrole solution at ice temperature and was stirred for an hour to reaction was accomplished. The fabricated nanocomposite was separated and purified as mentioned for polymerization of pyrrole. Five experiments with various amount of xanthan gum were conducted to produce the polypyrrole based nanocomposite that related details are given in Table 1.

3. Results and discussion

As mentioned above, nanocomposites were synthesized by various amount of xanthan gum that all details are given in Table 1. The electrical conductivity of PPy/XG nanocomposites using a standard four-probe method was considered. The results show that conductivity of synthesized nanocomposites was increased by increasing in amount of xanthan gum up to 0.904 S/cm with 2 g of xanthan gum. The increasing of polypyyrole based nanocomposite conductivity could be illustrated by carboxylate ion of xanthan gum. Carboxyl group presents in D-glucuronic acid and D-mannose unit which exist in side chain of xanthan gum that presence of lone pair electrons at oxygen atoms in carboxylic group probably can improve the electron mobility. However, by more increasing in amount of xanthan gum than 2 g conductivity of nanocomposites

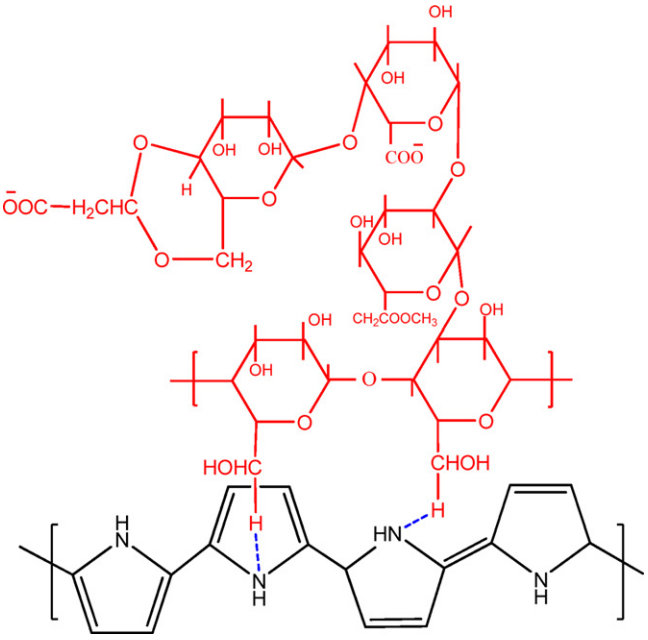

Fig. 2. The structural representation of the synthesized nanocomposite.

Table 2
FT-IR spectra of pure PPy, pure XG, nanocomposite No. 1, No. 2, and No. 3.

Nanocomposite No.	FT-IR spectra										
	COO^-		C=C	N—H	C=O	C=O	C—N	C—H	O—H	C—H	C—H
Pure XG	1615	1476	–	–	1568	1406	–	–	1023	1417	–
Pure PPy	–	–	1546	3425	–	–	1470	1176	–	–	1045
1	1600	1465	1539	3422	1560	1400	1463	1170	1030	1425	1049
2	1610	1470	1553	3439	1570	1403	1452	1164	1020	1420	1037
3	1617	1477	1576	3407	1565	1408	1475	1182	1024	1416	1052

was decreased to reach the electrical conductivity of pure xanthan gum.

FT-IR analyses were conducted to consider the chemical structure of substances. Fig. 1 shows the FT-IR spectrums of pure polypyrrole, xanthan gum and their composites. The *x*-axis represents wavelength (cm^{-1}) and *y*-axis display the light transmittance through the samples. For polypyyrole sample the peaks at 1546, 1470, 1176, 1045 and 3425 cm^{-1} can be observed that the band at 1546 is assigned to the pyrrole rings. The peaks at these bands indicate that the fabrication of polypyyrole was carried out [1–5]. In the case of xanthan gum FT-IR analysis two characteristic peaks were observed. One of them appears at 1615 cm^{-1} and the other at 1476 cm^{-1} which are attributed to COO^- groups. Additional bands of xanthan gum appear at 1417, 1023 cm^{-1} and 1568 cm^{-1} due to C—H, O—H and C=O bonds respectively [7]. The FT-IR spectra of nanocomposites reveal that all of the characteristic peaks of both xanthan gum and polypyyrole exist in the synthesized nanocomposites structure as the proposed structure is shown in Fig. 2. For example the synthesized nanocomposite No. 2 have characteristic bands at 1610, 1553, 3439, 1403, 1452, 1164, 1420 and 1020 cm^{-1} which are attributed to COO^- groups in xanthan gum, pyrrole rings, N—H group of polypyrrole, C=O in xanthan gum, C—N band of polypyrrole, C—H band of polypyrrole, C—H of xanthan gum and O—H band of xanthan gum structure respectively. All the characteristic peaks are reported in Table 2.

AFM imaging technique was employed in order to examine the surface morphology and roughness of PPy, XG and the fabricated nanocomposite. Fig. 3 shows the surfaces image of PPy, XG and synthesized nanocomposite in a scan size of 10 μm × 10 μm. The surface roughness parameters of the materials which are expressed in terms of the mean roughness (Sa), the root mean square of the *Z* data (Sq) and the mean difference between the five highest peaks and lowest valleys (Sz) were calculated from AFM images using tapping mode method via Nanosurf EasyScan software at a scan area of 10 μm × 10 μm that given in Table 3. As can be seen from the AFM images and reported parameters in Table 3 the surface roughness of nanocomposite is more than XG and less than pure PPy that it is probably due to the effect of XG on the structure of PPy. The obtained surface roughness parameters Sa, Sq and Sz of produced nanocamposite are 3467.1 pm, 4.78 nm and 69.53 nm respectively that reveal the surface of synthesized nanocomposite is more smooth than polypyrrole. The synthesized nanocomposites particle sizes measured by AFM device obtained from 58 to 98 nm that indicate xanthan gum decrease the average particle size of nanocomposite.

Table 3
Surface roughness parameters of pure XG, pure PPy and PPy/XG nanocomposite No. 2.

	Roughness parameters		
	Sa (pm)	Sq (nm)	Sz (nm)
Pure XG	1716.8	2.15	55.24
Pure PPy	4703.4	7.37	81.02
Nanocomposite No. 2	3467.1	4.78	69.53

Fig. 4 illustrates the results of thermogravimetric analysis of the PPy, XG and synthesized nanocomposites that done in the temperature range 0–800 °C. The thermogram of pure polypyyrole has three-step weight loss. The initial weight loss is due to the removal of adsorbed moisture. The small next weight loss can be observed attributed to loss volatile material. A third step shows a massive weight loss that it is owing to the degradation of the polymer chain. The thermogravimetric study of xanthan gum shows single step decomposition following on the small initial weight loss due to the removal of moisture. As seen the xanthan gum thermogram degradation temperature was found to be 280 °C. Weight loss continues to 50% then decreases as a char yield of 32% was achieved at 800 °C. In case of polypyyrole/xanthan gum nanocomposites, three steps weight loss can be seen. The first and second steps of weight loss were observed as polypyrrole thermogram due to removal of moisture and volatile materials. The third step weight loss which attributed to polymer chain decomposition begins in temperature higher than what was in xanthan gum thermal degradation. By comparing the thermograms of synthesized nanocomposites and pure polypyrrole one fact can be understand. It is the main effect of xanthan gum on thermal stability of produced nanocomposites that a remained ash amount is improved from 5 to 28%.

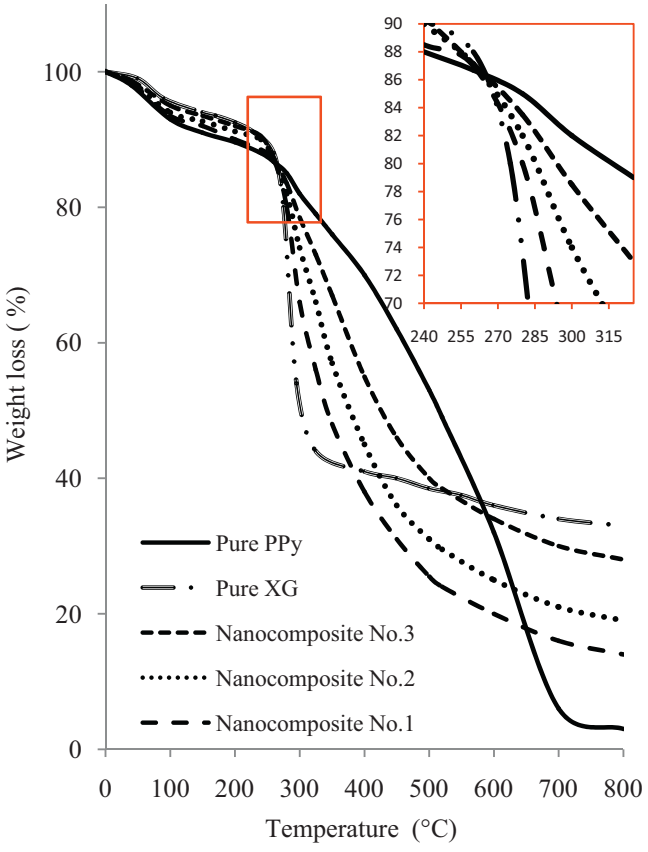

Fig. 4. TGA thermograms of pure PPy, pure XG, nanocomposite Nos. 1, 2 and 3.

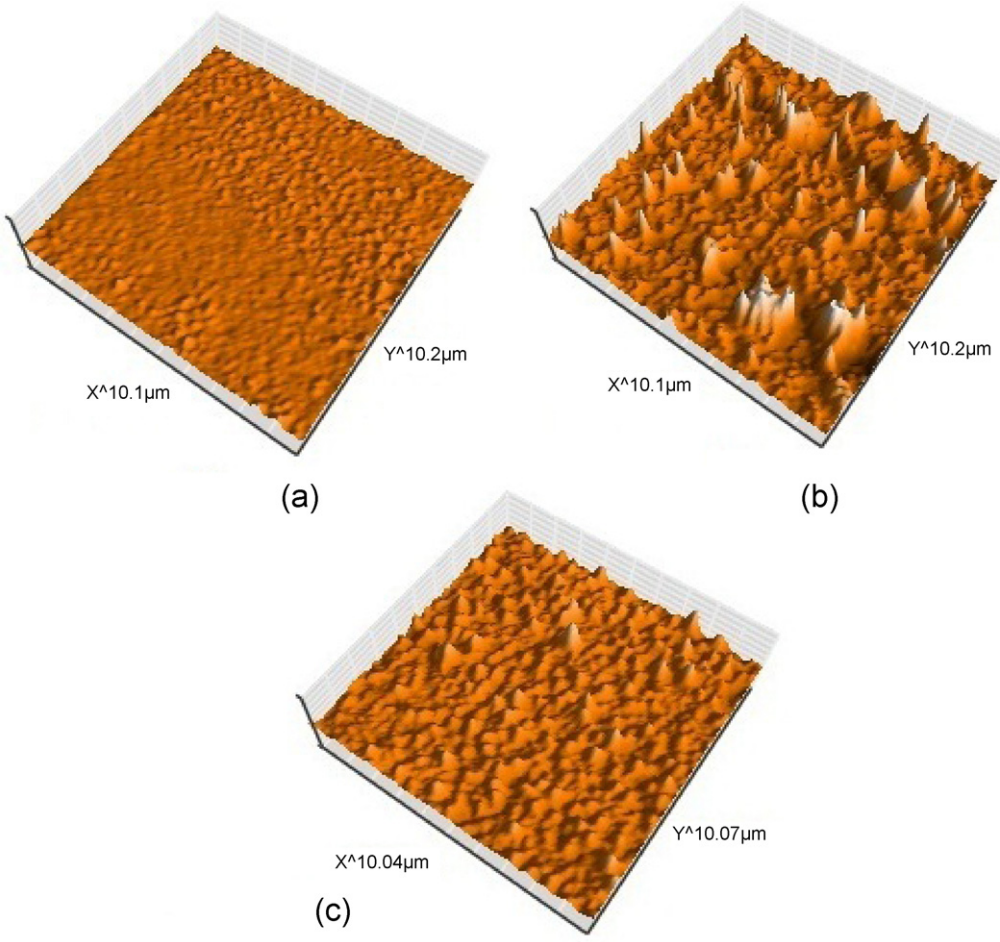

Fig. 3. AFM images of XG (a), PPy (b) and PPy/XG composite No. 2 (c) (image size = 10 μm × 10 μm).

4. Conclusions

In this work five runs by different amount of xanthan gum were performed to produce the nanocomposites of polypyrrole and xanthan gum by oxidative polymerization. Results showed that xanthan gum could enhance the electrical conductivity of polypyyrole from 0.537 S/cm (without xanthan gum) to 0.904 S/cm (with 2 g xanthan gum). However, the electrical conductivity of nanocomposite was decreased by increasing in amount of it more than 2 g. The morphology and chemical structure of synthesized nanocomposite were considered by AFM and FT-IR analyses. The AFM images of nanocomposites revealed that surface roughness of polypyyrole was intensively altered in presence of xanthan gum. The TGA analyses indicated that the thermal stability of synthesized nanocomposites was enhanced as a remained ash of substances was incremented by increasing in amount of xanthan gum.

References

[1] S. Yalcınkaya, C. Demetgul, M. Timur, N. Colak, Carbohydr. Polym. 79 (2010) 908–913.
[2] C. Yang, P. Liu, Synth. Met. 159 (2009) 2056–2062.
[3] A.G. Yavuz, A. Uygun, V.R. Bhethanabotla, Carbohydr. Polym. 81 (2010) 712–719.
[4] C. Sasso, D. Beneventi, E. Zeno, M. Petit-Conil, D. Chaussy, M.N. Belgacem, Synth. Met. 161 (2011) 397–403.
[5] J. Li, X. Qian, J. Chen, C. Ding, X. An, Carbohydr. Polym. 82 (2010) 504–509.
[6] R.P. Mikalo, G. Appel, P. Hoffmann, D. Schmeiber, Synth. Met. 122 (2001) 249–261.
[7] S.L. Gilani, G.D. Najafpour, H.D. Heydarzadeh, H. Zare, CI&CEQ 17 (2011) 179–187.
[8] H. Mirhosseini, C.P. Tan, N. Hamid, S. Yusof, Colloid Surf. A 315 (2008) 47–56.
[9] P.S. Gils, D. Ray, P.K. Sahoo, Int. J. Biol. Macromol. 45 (2009) 364–371.
[10] M.A. Ayadi, J.C. Leuliet, F. Chopard, M. Berthou, M. Lebouche, Food Bioprod. Process. 82 (2004) 320–325.
[11] W.S. Wan Ngah, L.C. Teong, M.A.K.M. Hanafiah, Carbohydr. Polym. 83 (2011) 1446–1456.
[12] H.C. Kang, K.E. Geckeler, Polymer 41 (2000) 6931–6934.
[13] H. Yuvaraj, M.H. Woo, E.J. Park, Y.T. Jeong, K.T. Lim, Eur. Polym. J. 44 (2008) 637–644.
[14] M. Sahin, Y. Sahin, A. Ozcan, Sens. Actuators B: Chem. 133 (2008) 5–14.
[15] J. Molina, J. Fernandez, A.I. Del rio, R. Lapuente, J. Bonastre, F. Cases, Polym. Degrad. Stabil. 95 (2010) 2574–2583.
[16] A.B. Slimane, C. Connan, M.G. Vaulay, M.M. Chehimi, Colloid Surf. A 332 (2009) 157–163.
[17] X. Xie, X. Zhou, Colloid Surf. A 386 (2011) 158–165.
[18] H. Zhao, W.E. Price, G.G. Wallace, J. Membr. Sci. 148 (1998) 161–172.
[19] X. Qi, C. Vetter, A.C. Harper, V.J. Gelling, Prog. Org. Coat. 63 (2008) 345–351.
[20] P. Wang, R. Lakis, A. MacDiarmid, Thin Solid Films 516 (2008) 2341–2345.
[21] N. Blinova, J. Stejskal, M. Trchova, J. Prokes, M. Omastova, Eur. Polym. J. 43 (2007) 2331–2341.
[22] A. Yfantis, G. Appel, D. Schmeißer, D. Yfantis, Synth. Met. 106 (1999) 187–195.